Available online at www.sciencedirect.com
ScienceDirect
Nuclear Instruments and Methods in Physics Research A 584 (2008) 273–284
NUCLEAR INSTRUMENTS & METHODS IN PHYSICS RESEARCH Section A
www.elsevier.com/locate/nima

Dual-readout calorimetry with lead tungstate crystals

N. Akchurin[a], L. Berntzon[a], A. Cardini[b], R. Ferrari[c], G. Gaudio[c], J. Hauptman[d], H. Kim[a], L. La Rotonda[e], M. Livan[c], E. Meoni[e], H. Paar[f], A. Penzo[g], D. Pinci[h], A. Policicchio[e], S. Popescu[i,1], G. Susinno[e], Y. Roh[a], W. Vandelli[c], R. Wigmans[a,*]

[a]*Texas Tech University, Lubbock, TX, USA*
[b]*Dipartimento di Fisica, Università di Cagliari and INFN Sezione di Cagliari, Italy*
[c]*Dipartimento di Fisica Nucleare e Teorica, Università di Pavia and INFN Sezione di Pavia, Italy*
[d]*Iowa State University, Ames (IA), USA*
[e]*Dipartimento di Fisica, Universitá della Calabria and INFN Cosenza, Italy*
[f]*University of California at San Diego, La Jolla, CA, USA*
[g]*INFN Trieste, Italy*
[h]*Dipartimento di Fisica, Università di Roma "La Sapienza" and INFN Sezione di Roma*
[i]*CERN, Genève, Switzerland*

Received 25 July 2007; received in revised form 4 September 2007; accepted 20 September 2007
Available online 7 October 2007

Abstract

Results are presented of beam tests in which a small electromagnetic calorimeter consisting of lead tungstate crystals was exposed to 50 GeV electrons and pions. This calorimeter was backed up by the DREAM Dual-Readout calorimeter, which measures the scintillation and Cherenkov light produced in the shower development, using two different media. The signals from the crystal calorimeter were analyzed in great detail in an attempt to determine the contributions from these two types of light to the signals, event by event. This information makes it possible to eliminate the dominating source of fluctuations and thus achieve an important improvement in hadronic calorimeter performance.

PACS: 29.40.Ka; 29.40.Vj

Keywords: Calorimetry; Cherenkov light; Lead tungstate crystals; Optical fibers

1. Introduction

High-precision measurements of hadrons and hadron jets have become increasingly important in experimental particle physics. Such measurements are considered a crucial ingredient of experiments at a future high-energy Linear Electron-Positron Collider. Historically, by far the best performance in this respect has been delivered by *compensating* hadron calorimeters [1]. In these instruments, the response to the electromagnetic (em) and non-electromagnetic shower components is equalized by design, and therefore the detrimental effects of event-to-event fluctuations in the energy sharing between these components are eliminated. These effects include hadronic signal non-linearity, a poor hadronic energy resolution, especially at high energies where deviations from $E^{-1/2}$ scaling become the dominant factor, and a non-Gaussian response function.

In recent years, an alternative technique has been developed: The Dual Readout Method (DREAM). DREAM calorimeters offer the same advantages as compensating ones, and are not subject to the disadvantages of the latter. These disadvantages derive from the fact that compensation can only be achieved in sampling calorimeters with a small sampling fraction (e.g., 2.3% in

*Corresponding author. Fax: +1 806 742 1182.
E-mail addresses: wigmans@ttu.edu, Richard.Wigmans@ttu.edu (R. Wigmans).
[1]On leave from IFIN-HH, Bucharest, Romania.

0168-9002/$ - see front matter © 2007 Elsevier B.V. All rights reserved.
doi:10.1016/j.nima.2007.09.035

lead/plastic-scintillator), plus the fact that compensation relies upon efficient detection of the neutrons produced in the shower development. These requirements limit the em energy resolution achievable with these instruments, while the excellent hadronic performance is only achieved with sufficiently large detector volumes and integration times.

DREAM calorimeters are based on a simultaneous measurement of different types of signals which provide complementary information about details of the shower development. The first calorimeter of this type that we developed and tested (in the context of a generic R&D project) was based on a copper absorber structure, equipped with two types of active media. Scintillating fibers measure the total energy deposited by the shower particles, while Cherenkov light is only produced by the charged, relativistic shower particles. Since the latter are almost exclusively found in the em shower component (dominated by π^0s produced in hadronic showers), a comparison of the two signals makes it possible to measure the energy fraction carried by this component, f_{em}, event by event. As a result, the effects of fluctuations in this component, which are responsible for all traditional problems in non-compensating calorimeters, can be eliminated. This leads to an important improvement in the hadronic calorimeter performance. The performance characteristics of this detector are described elsewhere [2–4].

Once the effects of the dominant source of fluctuations, i.e., fluctuations in the em energy fraction f_{em}, are eliminated, the performance characteristics are determined (and limited) by other types of fluctuations. In the described detector, a prominent role was played by the small number of Cherenkov photoelectrons constituting the signals (8 p.e./GeV). However, there is absolutely no reason why the DREAM principle would only work in fiber calorimeters, or even in sampling calorimeters for that matter. One could in principle even use a homogeneous (fully sensitive) detector, provided that the light signals can be separated into scintillation and Cherenkov components. In this paper, we describe the results of tests of this idea. A small electromagnetic calorimeter made of lead tungstate ($PbWO_4$) crystals was tested in conjunction with the DREAM calorimeter mentioned above, and exposed to high-energy particle beams at CERN's Super Proton Synchrotron.

In Section 2, we describe the detectors and the experimental setup in which they were tested. In Section 3, we discuss the experimental data that were taken and the methods used to analyze these data. In Section 4, the experimental results are described and discussed. A summary and conclusions are presented in Section 5.

2. Detectors and experimental setup

2.1. Detectors

The calorimeter system used in these experiments comprised two sections. The electromagnetic section (ECAL) consisted of 19 lead tungstate ($PbWO_4$) crystals.[2] Each crystal was 18 cm long, with a cross section of $2.2 \times 2.2\,\mathrm{cm}^2$. These crystals were arranged in a matrix, as shown in Fig. 1.

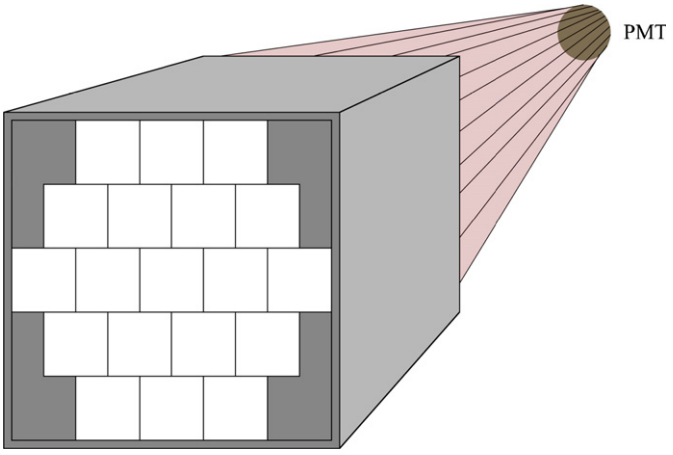

Fig. 1. The lead tungstate electromagnetic section of the calorimeter system.

For the purpose of these tests, this ensemble of crystals was considered one unit. The crystals were not optically isolated from each other, and the light produced by showering particles was read out by only two photomultiplier tubes (PMT),[3] one located at each end of the crystal matrix. The light was funneled into these tubes by means of cones made of aluminized mylar, a highly reflective material.

For the hadronic section (HCAL) of the calorimeter system, we used the original DREAM calorimeter [2–4]. The basic element of this detector is an extruded copper rod, 2 m long and $4 \times 4\,\mathrm{mm}^2$ in cross section. This rod is hollow, and the central cylinder has a diameter of 2.5 mm. Seven optical fibers were inserted in this hole. Three of these were plastic scintillating fibers, the other four fibers were undoped fibers, intended for detecting Cherenkov light. The instrumented volume had a length of 2.0 m ($10\lambda_{\mathrm{int}}$, 100 X_0), an effective radius of 16.2 cm and a mass of 1030 kg.

The fibers were grouped to form 19 hexagonal towers. The effective radius of each tower was 37.1 mm ($1.82\rho_M$). A central tower (#1) was surrounded by two hexagonal rings, the Inner Ring (six towers, numbered 2–7) and the Outer Ring (12 towers, numbered 8–19). The towers were longitudinally unsegmented. The fibers sticking out at the rear end of this structure were separated into 38 bunches: 19 bunches of scintillating fibers and 19 bunches of Cherenkov fibers. In this way, the readout structure was established. Each bunch was coupled through a 2 mm air

[2] On loan from the ALICE Collaboration, who use these crystals for their PHOS calorimeter.

[3] Hamamatsu R5900U, 10-stage.

gap to a PMT.[4] More information about this detector is given elsewhere [2,3].

2.2. The beam line

The measurements described in this paper were performed in the H4 beam line of the Super Proton Synchrotron at CERN. The detectors were mounted on a platform that could move vertically and sideways with respect to the beam. The ECAL was rotated into different positions (see Section 4) by hand. Two small scintillation counters provided the signals that were used to trigger the data acquisition system. These Trigger Counters were 2.5 mm thick, and the area of overlap was $6 \times 6\,cm^2$. A coincidence between the logic signals from these counters provided the trigger.

2.3. Data acquisition

Measurement of the time structure of the calorimeter signals formed a very important part of the tests described here. In order to limit distortion of this structure as much as possible, we used 15 mm thick air-core cables to transport the ECAL signals to the counting room. Such cables were also used for the signals from the trigger counters, and these were routed such as to minimize delays in the DAQ system.[5]

The HCAL signals were transported through RG-58 cables with (for timing purposes) appropriate lengths to the counting room. The ECAL signals were split (passively) into five equal parts in the counting room. One part was sent to a charge ADC, the other four signals were used for analysis of the time structure by means of a FADC. The latter unit measured the amplitude of the signals at a rate of 200 MHz. During a time interval of 80 ns, 16 measurements of the amplitude were thus obtained. The four signals from the splitter box were measured separately in four different channels of the FADC module.[6] Signals 2, 3 and 4 were delayed by 1.25, 2.50 and 3.75 ns with respect to signal 1. By using four channels of the FADC module in this way, the time structure of the signals was thus effectively measured with a resolution of 1.25 ns (800 MHz).

The quality of the information obtained in this way is illustrated in Fig. 2, which shows the average time structure of the signals from 50 GeV electron showers developing in the lead tungstate ECAL. The trailing edge of these signals is well described by an exponential decay with a time constant of 9.7 ns.

The charge measurements were performed with 12-bit LeCroy 1182 ADCs. These had a sensitivity of 50 fC/count and a conversion time of 16 μs. The ADC gate width was

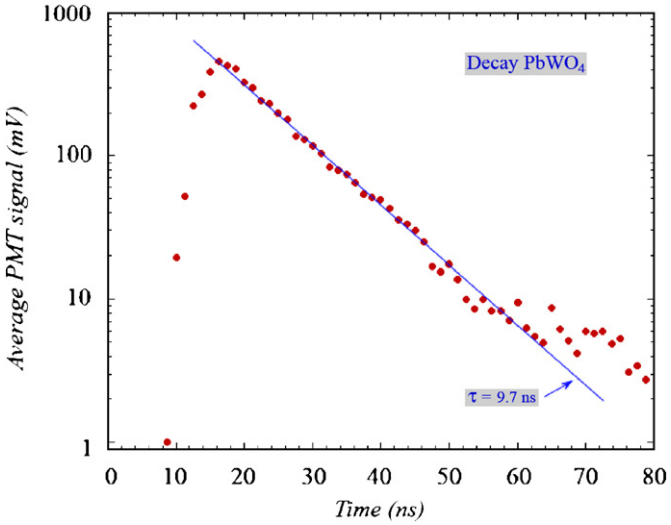

Fig. 2. Average time structure of the signals from 50 GeV electron showers in the lead tungstate crystals.

100 ns, and the calorimeter signals arrived ~20 ns after the start of the gate.

The data acquisition system used VME electronics. A single VME crate hosted all the needed readout and control boards. The trigger logic was implemented through NIM modules and the signals were sent to a VME I/O register, which also collected the spill and the global busy information. The VME crate was linked to a Linux based computer through an SBS 620[7] optical VME-PCI interface that allowed memory mapping of the VME resources via an open source driver.[8] The computer was equipped with a 2 GHz Pentium-4 CPU, 1 GB of RAM, and was running a CERN SLC 4.3 operating system.[9]

The data acquisition was based on a single-event polling mechanism and performed by a pair of independent programs that communicated through a first-in-first-out buffer, built on top of a 32 MB shared memory. Only exclusive accesses were allowed and concurrent requests were synchronised with semaphores. The chosen scheme optimized the CPU utilization and increased the data taking efficiency by exploiting the bunch structure of the SPS, where beam particles were provided to our experiment during a spill of 4.8 s, out of a total cycle time of 16.8 s. During the spill, the readout program collected data from the VME modules and stored them into the shared memory, with small access times. During the remainder of the SPS cycle, a recorder program dumped the events to the disk. Moreover, the buffer presence allowed low-priority monitoring programs to run (off-spill) in spy mode. With this scheme, we were able to reach a data acquisition rate as high as 2 kHz, limited by the

[4]Hamamatsu R-580, 10-stage, 1.5 in. diameter, bialkali photocathode, borosilicate window.

[5]We measured the signal speed to be $0.78c$ in these cables.

[6]Dr. Struck SIS3320, http://www.struck.de/sis3320.htm

[7]http://www.gefanucembedded.com/products/457

[8]http://www.awa.tohoku.ac.jp/~sanshiro/kinoko-e/vmedrv/

[9]http://linux.web.cern.ch/linux/scientific4/

FADC readout time. The typical event size was ~1 kB. All calorimeter signals and the signals from the auxiliary detectors were monitored on-line.

2.4. Calibration of the detectors

The two PMTs reading out the two sides of the ECAL were calibrated with 50 GeV electrons. To this end, the ECAL was oriented such that the beam entered the detector perpendicular to the crystal axis, and the two PMTs collecting the light generated by the showers were located in a plane perpendicular to the beam axis (Fig. 3). The main purpose of this setup was to equalize the gain of the two PMTs in a geometry where the relative contributions of scintillation and Cherenkov light to the signals were the same for both. Given the radiation length of $PbWO_4$ (8.9 mm), the ECAL was only $12.4X_0$ deep in this geometry, and therefore, a substantial fraction of the shower energy leaked out. The energy equivalent of the signals thus had to be established on the basis of (EGS4) Monte Carlo simulations.

The 38 PMTs reading out the 19 towers of the HCAL were also all calibrated with 50 GeV electrons. The showers generated by these particles were not completely contained in a single calorimeter tower. The (average) containment was found from EGS4 Monte Carlo simulations. When the electrons entered a tower in its geometrical center, on average 92.5% of the scintillation light and 93.6% of the Cherenkov light was generated in that tower [2]. The remaining fraction of the light was shared by the surrounding towers. The signals observed in the exposed tower thus corresponded to an energy deposit of 46.3 GeV in the case of the scintillating fibers and of 46.8 GeV for the Cherenkov fibers. This, together with the precisely measured values of the average signals from the exposed tower, formed the basis for determining the calibration constants, i.e., the relationship between the measured number of ADC counts and the corresponding energy deposit.

3. Experimental data

The main purpose of these tests was to see if the ECAL signals could be split into their scintillation and Cherenkov components. In order to optimize the possibilities in this respect, the ECAL was oriented such that the angle between the crystal axis and the beam axis was equal to the Cherenkov angle, θ_C:

$$\cos\theta_C = 1/n \quad (1)$$

Since the refractive index of $PbWO_4$ is 2.2, $\theta_C \approx 63^\circ$. Detailed measurements of the angular dependence of the Cherenkov/scintillation ratio [5] revealed indeed a maximum value near $\theta = 63^\circ$, and therefore we chose this angle for our tests. The detector setup is shown in Fig. 4. In this geometry, the effective depth of the ECAL amounted to $12.4/\sin\theta_C \sim 14X_0$, and it contained on average ~90% of 50 GeV electron showers. The remaining 10% of the shower energy was recorded in the HCAL.

We exposed the calorimeter system to 50 GeV electrons and to 50 and 100 GeV π^+. For each run,100 000 events were collected. The time structure of both ECAL signals was measured with 1.25 ns resolution. The integrated charge carried by these signals and by those from the 38 HCAL channels was digitized with 12 bit resolution.

The beams turned out to be very clean. Contamination in the electron beam was less than 10^{-4}. The pion beams contained muons, at the few-% level. These muons could be easily recognized and removed from the event samples. We used the muon events for separate studies.

4. Experimental results

4.1. Forward/backward asymmetry

In lead tungstate, sufficiently relativistic charged shower particles emit Cherenkov light at an angle of 63°. Unlike the scintillation light, which is isotropically emitted, there is a clear directional preference in the Cherenkov light

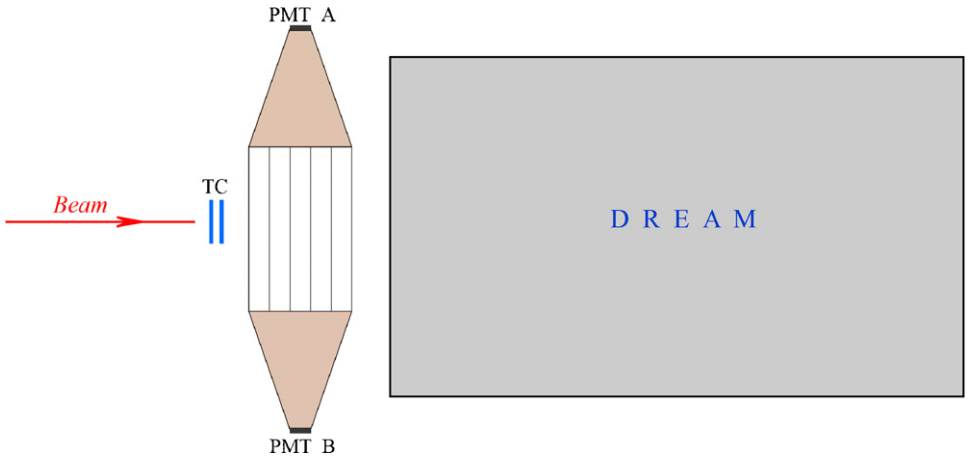

Fig. 3. The detector setup used for calibrating the ECAL channels (PMTs A and B).

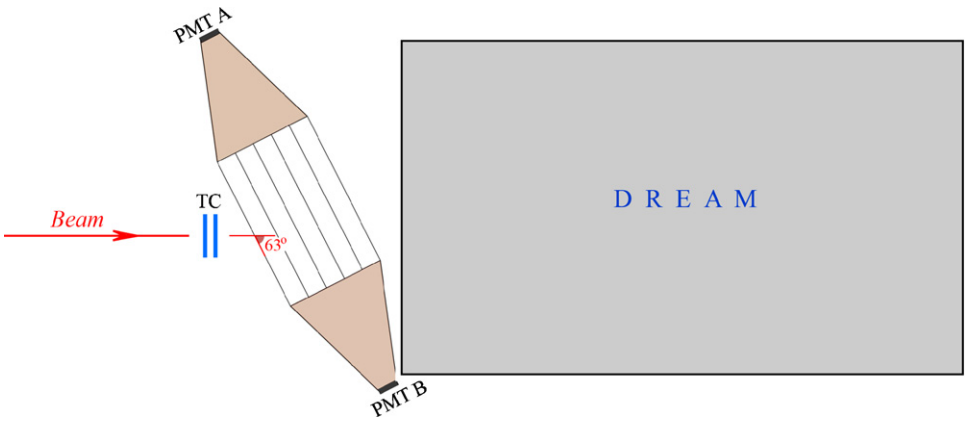

Fig. 4. The detector setup used for studying the Cherenkov contributions to the ECAL signals.

production of high-energy showers. Even though much of the shower energy is deposited by isotropically distributed electrons, produced in Compton scattering and photoelectric processes, the effects of that on the angular distribution of the emitted Cherenkov light are limited, since much of this takes place below the Cherenkov threshold ($p_e = 0.26\,\mathrm{MeV}/c$). Quantitative information on this was obtained from the angular dependence of the response of quartz-fiber calorimeters (which are exclusively detecting Cherenkov light) to high-energy electron showers [6]. The maximum response was obtained when the fibers were oriented at the Cherenkov angle with respect to the shower axis. This response was reduced by a factor 2–3 when the fibers were aligned with the beam axis, and by a factor 10 when read out at the upstream end.

We are exploiting this feature by comparing the signals from the two ECAL channels in the 63° geometry (Fig. 4). Any Cherenkov light produced in the shower development will be preferentially observed in the downstream channel (to be named channel B in the following), whereas the upstream channel (channel A) will see a much smaller fraction of it. Since both PMTs see the same amount of scintillation light, the *forward/backward asymmetry*, $(B-A)/(B+A)$, is a measure for the fraction of Cherenkov light contained in the signals.[10]

Fig. 5a shows the measured asymmetry for the 50 GeV electron signals from the ECAL. Indeed, the B signals are significantly larger than the A ones, on average by ~9%. The forward/backward asymmetry was measured to be $4.4 \pm 0.1\%$. Forward/backward asymmetry was also observed in the ECAL signals from pions and muons. The muon asymmetry is shown in Fig. 5b. The asymmetry is larger than for electron showers, the B signals were measured to be, on average, larger by ~20% than the A ones (the forward/backward asymmetry was measured to be $10.4 \pm 1.0\%$). However, the event-to-event fluctuations are considerably larger. The σ_{rms} of the distribution for muons is larger by a factor 35–40 than the width of the distribution for electron showers. The latter phenomenon is due to the fact that the electron signals are considerably larger (45 GeV vs. 0.1 GeV for a mip), so that Poisson fluctuations in the number of photoelectrons account for at least half of this difference.[11] In addition, because of the Landau distribution of the muon signals, these statistical fluctuations are non-Poissonian for these particles.

The larger average asymmetry for muons should be expected on the basis of the fact that Cherenkov light generated in em showers contains an isotropic component, mainly produced by Compton electrons [1]. In a separate paper, we have shown that measurements of em showers in thin $PbWO_4$ crystals revealed that the forward/backward asymmetry decreases as the em shower develops. In the first $2-3X_0$, an asymmetry of ~7% was measured, but this asymmetry decreased considerably when deeper regions of the shower were probed. The asymmetries measured here for complete em showers and for single particles (muons) are in complete agreement with these observations.

After removing the (6%) muons from the 50 GeV hadronic event sample, the remaining pion events exhibited some interesting characteristics, which are a direct consequence of the large e/h ratio of the $PbWO_4$ crystal calorimeter.[12] Figs. 6a and 6b show the total signal distributions in the HCAL and ECAL, respectively. The HCAL distributions exhibits a structure that is the sum of two distinct substructures, as illustrated in Figs. 6c and 6d. Fig. 6c shows the HCAL distribution for pions that penetrated the ECAL. These events populate the mip peak in the ECAL distribution. The fact that these pions represent 40% of the total means that the ECAL's thickness in this geometry corresponded to $-\ln 0.6 = 0.5$ nuclear interaction lengths.

The pion events were subdivided into samples depending on the total signal produced in the ECAL. The

[10] We measured that the $(B-A)/(B+A)$ ratio of the scintillation component of the signal changed by less than 0.5% as a result of rotating the crystal matrix. Details of this measurement are given in Section 4.2.

[11] A Gaussian fit to the distribution from Fig. 5b gave a σ of 0.60. If (Poisson) photoelectron statistics was the only contributing factor to the width, one should expect a sigma of 0.46.

[12] This e/h value was measured to be 2.4 [7].

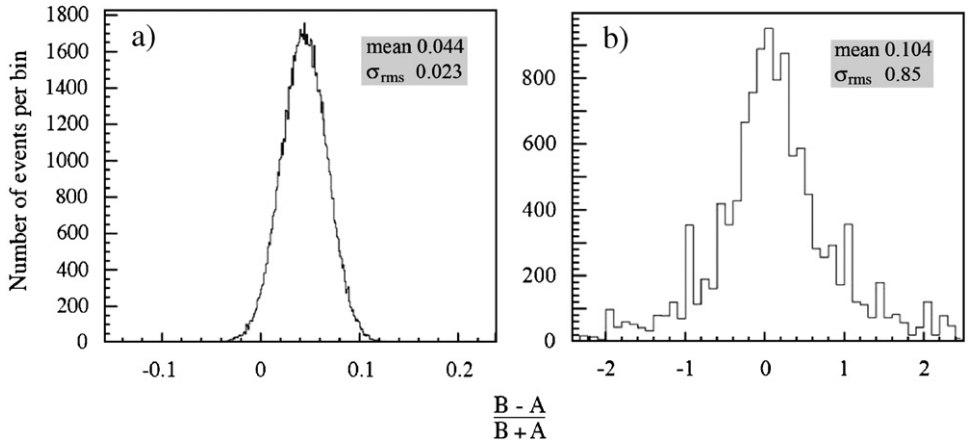

Fig. 5. Distribution of the Forward/Backward asymmetry for 50 GeV electron signals (a) and 50 GeV μ^+ signals (b) in the lead tungstate ECAL.

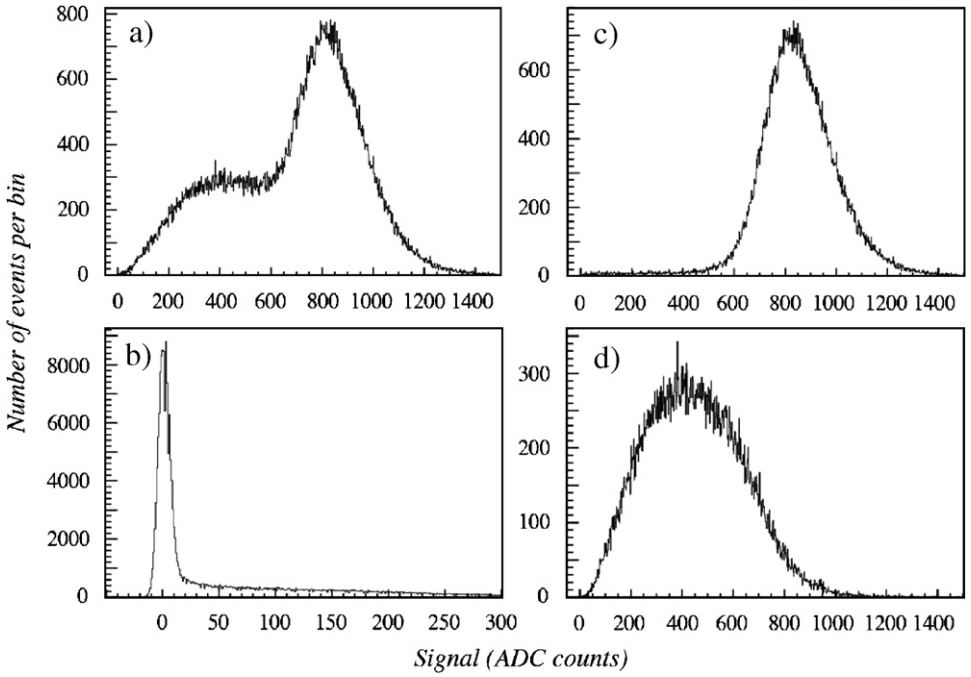

Fig. 6. Signal distributions for 50 GeV π^+ in the ECAL/HCAL system. Shown are the total signal distributions in the HCAL (a) and in the ECAL (b), as well as the signal distributions in HCAL for pions that gave a mip signal in the ECAL (c) and for pions that produced a larger signal in the ECAL (d). The HCAL signals concern the scintillating fibers only.

underlying idea is that the relatively thin ECAL will, for all practical purposes, only contain the remnants of the first generation of nuclear reactions in the hadronic shower development. If the first interaction took place in the first two crystals of the ECAL, then π^0s produced in this first interaction typically deposited most of their energy in the ECAL. Therefore, one should expect a correlation between the total ECAL signal and the fraction of Cherenkov light. Fig. 7 clearly exhibits such a correlation. By comparing the results shown in Figs. 5a and 7, the average fraction of the ECAL signal carried by em shower components may be determined.

However, this determination is complicated by another effect shown in Fig. 7, namely the Landau tail of pions penetrating the ECAL. Not surprisingly, the events in the mip peak of the pion distribution exhibit the same asymmetry as the muons from our sample: $10.5 \pm 0.3\%$, where the smaller error reflects the difference in event statistics. However, event samples with signals larger than the mip peak in the ECAL do contain some fraction of penetrating pions, from the Landau tail. Because of the much larger asymmetry for such events, the overall asymmetry for these event samples is measurably affected. A similar effect may be expected for events in which the first pion interaction

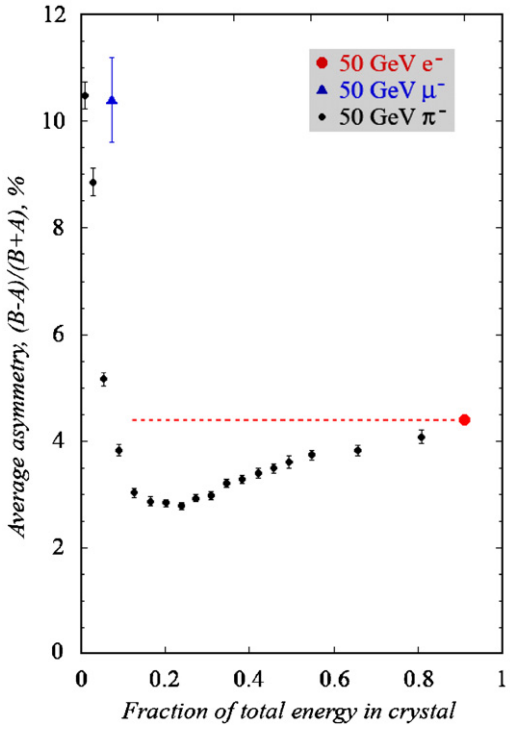

Fig. 7. Average Forward/Backward asymmetry for 50 GeV pion signals in the lead tungstate ECAL, as a function of the energy fraction deposited by the beam particles in this detector.

occurred deep inside the ECAL. Measurements with a single crystal indicated that em showers developing only over a few radiation lengths exhibit an asymmetry of ~7%, i.e., not much smaller than that for mips [5].

As a result of these complications, the measured asymmetry starts to reflect the em component of the hadron showers only for events in which at least 10 GeV (20% of the total energy) was deposited in the ECAL.

In order to check the latter statement, we investigated the relationship between the Cherenkov components of the signals observed in the em and hadronic sections of our calorimeter system. In order to limit the contaminating effects of the penetrating pions, we limited this study to pions that deposited more than 10 GeV in the ECAL. The relative contribution of Cherenkov light to the signals was derived from the $(B-A)/(B+A)$ asymmetry in the ECAL and from the Q/S signal ratio in the DREAM hadronic section. Fig. 8 shows that there is a clear correlation between these quantities. And since the Q/S signal ratio is directly related to the em shower fraction, f_{em}, we conclude from this that the asymmetry measured in the ECAL is indeed an indicator for the fraction of the ECAL signal carried by the em shower component.

This can also be seen as follows. If we denote the ECAL Cherenkov signal by Q and the scintillation signal by S, as in the DREAM hadronic section, then the

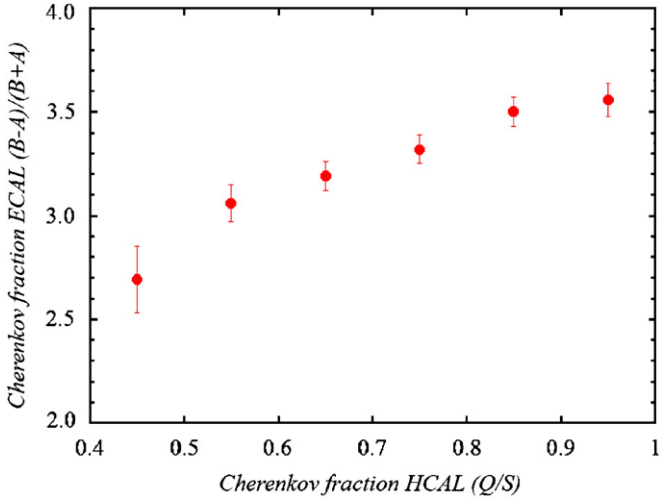

Fig. 8. Correlation between the average fractions of Cherenkov light measured in the ECAL and HCAL signals, for 50 GeV pions starting their showers in the ECAL, and depositing at least 10 GeV in the crystals.

forward/backward asymmetry in the ECAL signals can be written as

$$\frac{B-A}{B+A}=\frac{Q}{2S+Q} \tag{2}$$

Since in practice $Q \ll S$, the asymmetry is approximately equal to 0.5 Q/S, and therefore the asymmetry is related in a similar way to f_{em} as the Q/S signal ratio measured for the DREAM hadronic section. In Reference [3], we derived the exact relationship between Q/S and f_{em} for DREAM:

$$\frac{Q}{S}=\frac{f_{em}+0.21(1-f_{em})}{f_{em}+0.76(1-f_{em})} \tag{3}$$

where the factors 0.21 and 0.76 are the inverse values of the e/h ratios of the Cu/quartz and Cu/plastic-scintillator sampling structures, respectively. A similar relationship can be derived between the forward/backward signal asymmetry and the em shower fraction in ECAL. Two modifications of Eq. (3) are important:

(1) The e/h value of ECAL as a scintillation device is much larger than for the Cu/plastic sampling structure in DREAM: 2.4 vs. 1.3
(2) Since the scintillation and Cherenkov signals of the ECAL are not independently calibrated, as in DREAM, an overall calibration factor is needed that relates the strengths of the Q and S signals in ECAL. This factor is such that the asymmetry is 0.044 for $f_{em}=1$ (pure em showers, see Fig. 5).

These considerations lead to the following relationship between the measured forward/backward asymmetry in the ECAL signals (with the detector oriented at the Cherenkov angle) and the em fraction of the shower energy deposited

in this calorimeter section:

$$\frac{B-A}{B+A} = 0.044\frac{f_{em}+0.21(1-f_{em})}{f_{em}+0.42(1-f_{em})} \quad (4)$$

This relationship is graphically shown in Fig. 9. The same figure also shows (on the top horizontal axis) the Q/S ratio in the fiber calorimeter section. If the experimental data points were located on this curve, we would conclude that the em shower fraction derived from the em and hadronic signal characteristics was *exactly* the same. However, since the crystal and the fiber sections of the calorimeter system probed different parts of the shower development, and especially since the crystal section only probed the first 0.5 nuclear interaction lengths, such a perfect one-to-one correspondence should not be expected. However, Fig. 9 does show a clear correlation between the em shower fractions derived from both detector segments.

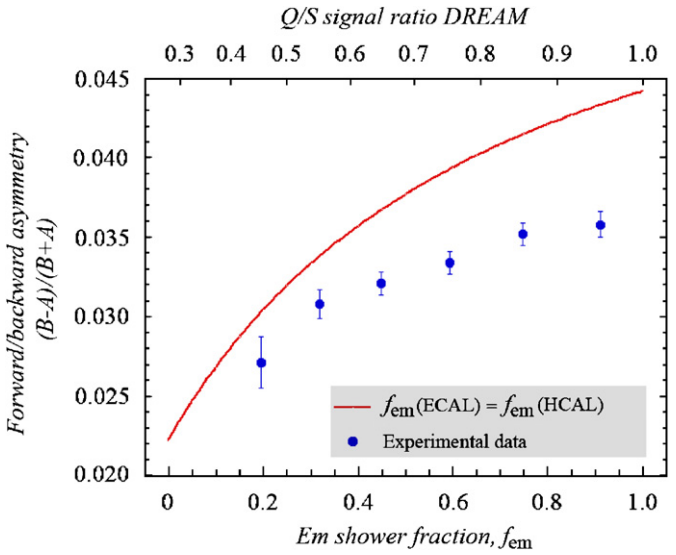

Fig. 9. Relationship between measured quantities and the em shower fraction. The measured quantities concern the Q/S signal ratio measured in the DREAM hadronic section (top horizontal axis) and the forward/backward signal asymmetry measured in the crystal ECAL (vertical axis).

The practical merits of all this were studied by investigating the relationship between the asymmetry in the ECAL signals and the *total* response of the calorimeter system (ECAL + HCAL), for this event sample. We recall that in DREAM, there is a direct relationship between the Q/S signal ratio, i.e., the ratio of the total signals measured in the Cherenkov fibers and the scintillation fibers, and the em shower fraction, f_{em} [3]. By selecting events with a certain Q/S value, the f_{em} value is fixed. The total calorimeter signal for these events is different from that for events with a different Q/S, and thus f_{em} value.

This is illustrated in Fig. 10, which shows in diagram *b* two signal distributions for event samples with very different Q/S values. The Q/S bins used for these samples are shown in Fig. 10a. The events selected for this purpose all concern pions that penetrated the ECAL without a

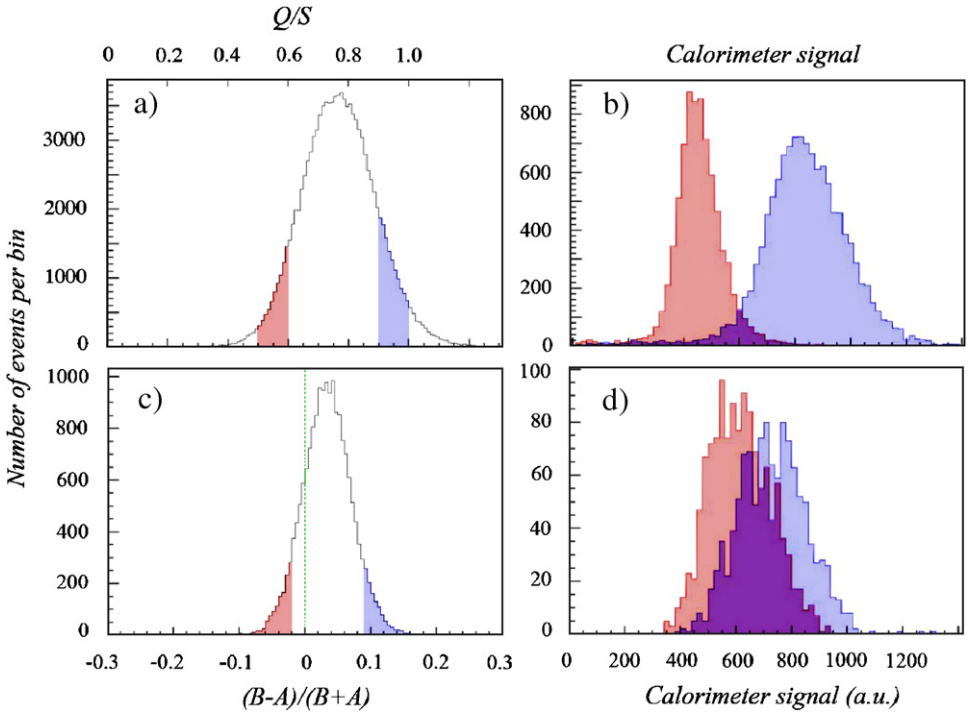

Fig. 10. Total calorimeter signal distribution for 50 GeV π^+ (right), for different choices of variables that select the em shower content (left). Diagram b shows the total quartz signal for two different Q/S bins, indicated in diagram a, for pions that penetrated the crystal ECAL. In diagram (d) the distribution of the sum of the DREAM scintillator signals and crystal signal B is displayed, for two different choices of the ECAL asymmetry parameter, shown in diagram (c). The latter distributions concern events in which at least 10 GeV was deposited in the ECAL.

nuclear interaction. Therefore, almost all the energy carried by these pions was deposited in the fiber calorimeter section. These results illustrate that a larger em shower fraction (selected by means of the Q/S signal ratio) leads to a considerably larger total calorimeter signal, especially in the extremely non-compensating copper/quartz-fiber structure ($e/h = 4.7$) used for this purpose.

In Fig. 10d, two signal distributions are shown for events that were selected on the basis of the forward/backward asymmetry measured in the ECAL crystal section. The $(B-A)/(B+A)$ bins used for these two samples are shown in Fig. 10c. Only events in which the pions deposited at least 10 GeV in the crystal were used for this purpose, and the total signal was calculated as the sum of the signal measured in PMT B and the signal from the scintillating fibers in the hadronic section. These results exhibit, at least qualitatively, the same characteristics as those shown above for the penetrating pions, where the Q/S ratio provided information on f_{em}: the larger the asymmetry measured in the ECAL signal, i.e., the larger the relative contribution of Cherenkov light to the ECAL signals, the larger the em shower fraction, and thus the larger the total calorimeter signal becomes.

In Fig. 11, the described phenomena are shown for the entire range of possible f_{em} values. The total calorimeter signal for penetrating events (mip in ECAL) is plotted as a function of the Q/S value in Fig. 11a, and in Fig. 11b as a function of the $(B-A)/(B+A)$ value for pions interacting in the ECAL (and depositing more than 10 GeV in the crystals).

A few remarks are in order. The fact that the effect shown in Fig. 11a (which we will call the *reference effect*) is much larger than that in Fig. 11b can be ascribed to two factors:

(1) The reference effect concerns exclusively Cherenkov light. We are looking at the total Cherenkov signal as a function of f_{em}. Had we chosen the signals from the scintillating fibers instead, the observed increase in the calorimeter response would have been only 15%, instead of the factor of two measured for the Cherenkov reponse [3]. This is a consequence of the very large difference between the e/h values (4.7 vs. 1.3), which forms the very basis of the DREAM principle [8]. For the em content derived on the basis of the forward/backward asymmetry in the crystal signals, we do not have the option to look exclusively at Cherenkov light. A very large fraction of the signal from the crystals consists of scintillation light, even if we optimize the event selection for em shower content, i.e., Cherenkov contributions.
(2) The ECAL is only $14X_0$ deep. Even though much of the em component of hadron showers derives from π^0 production in the first nuclear interaction of the showering particle, the measurement of f_{em} for the entire shower on the basis of the signals from the first $14X_0$ has its limitations.

In light of these considerations, the effect observed in Fig. 11b is actually quite remarkable, although it should also be pointed out that, since the e/h value of a homogeneous $PbWO_4$ calorimeter is ~2.4, a larger increase than the 15% mentioned above should be expected for the combination considered here. Fig. 12 summarizes the

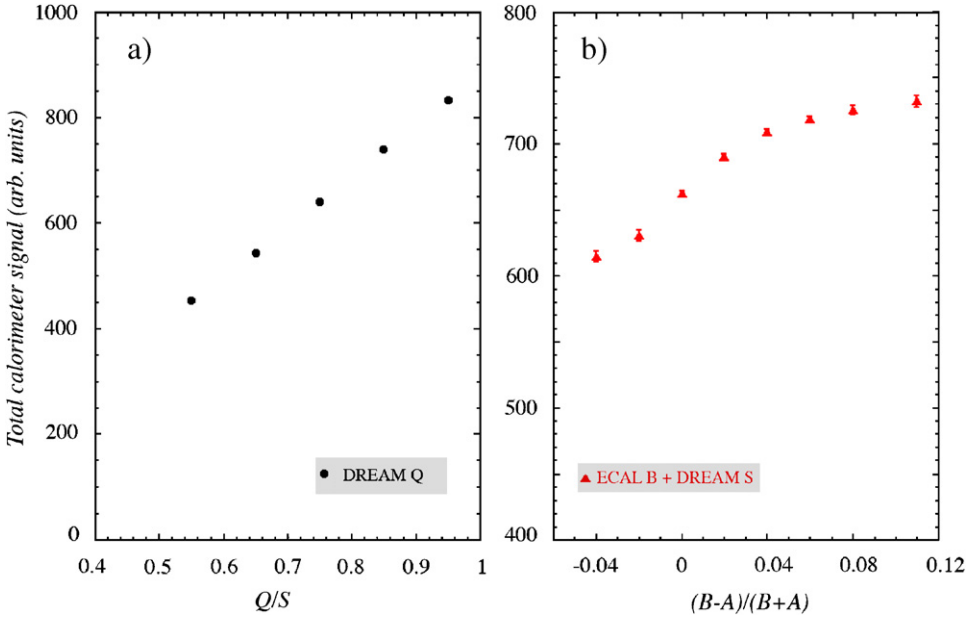

Fig. 11. Average total calorimeter signal for 50 GeV π^+, as a function of variables that select the em shower content. Diagram a shows the total quartz signal as a function of the Q/S signal ratio, for pions that penetrated the crystal ECAL. In diagram b the sum of the DREAM scintillator signals and the downstream crystal signal (B) is displayed, for events in which at least 10 GeV was deposited in the ECAL.

non-linearity characteristics for the different signals and signal combinations. Since the calorimeter response (R) can be written schematically as (3)

$$R = f_{em} + (1 - f_{em})h/e \quad (5)$$

it is a linear function of the em shower fraction, with an intercept determined by the (inverse of the) e/h value:

$$R = h/e + (1 - h/e)f_{em} \quad (6)$$

This relationship is represented by the straight lines in Fig. 12.

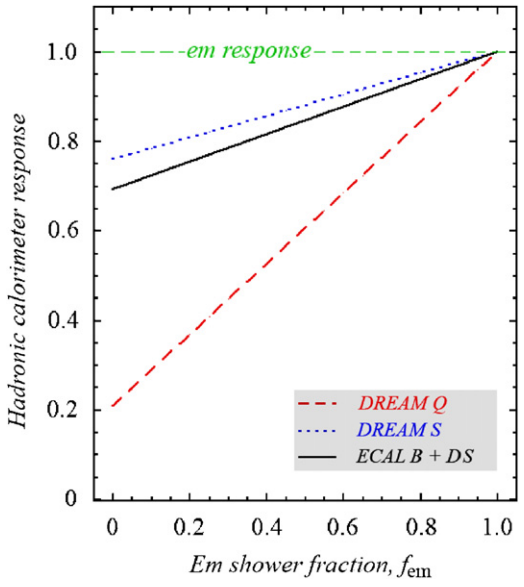

Fig. 12. The hadronic calorimeter response as a function of f_{em} for different signals and signal combinations, which reflect the degree of non-compensation. See text for details.

We also want to point to another difference between the data sets shown in Figs. 11a and 11b. As explained in Ref. [3], there is a linear relationship between f_{em} and the total calorimeter signal. Even though the parameters Q/S and $(B-A)/(B+A)$ are not exactly proportional to f_{em}, it is remarkable that the signal dependence for Q/S is approximately linear, while it is not for $(B-A)/(B+A)$. This may be explained from the fact that the latter curve extends beyond the physically meaningful region, $0<f_{em}<1$, contrary to the Q/S curve. This region is limited to $0<(B-A)/(B+A)<0.044$, and the points outside this region probe the tails of the distribution. This may explain the "S- shaped" curve of Fig. 11b. A similar deviation from linearity is actually also observed if points covering the unphysical region $Q/S>1$ are included in Fig. 11a.

4.2. Time structure of the ECAL signals

A second valuable tool for recognizing the contributions of Cherenkov light to the calorimeter signals is derived from the time structure of the events. This is illustrated in Fig. 13, which shows the average time structure of the 50 GeV shower signals recorded with the same PMT (B) in the two geometries shown in Figs. 3 and 4. The two distributions have been normalized on the basis of their trailing edge (24–80 ns after the start of the FADC digitization), and are indeed in great detail identical in that domain, both for the electron (Fig. 13c) and for the pion (Fig. 13d) signals. This part of the pulses is completely determined by the decay characteristics of the scintillation processes in the $PbWO_4$ crystals (see also Fig. 2) and should thus be independent of the detector orientation.

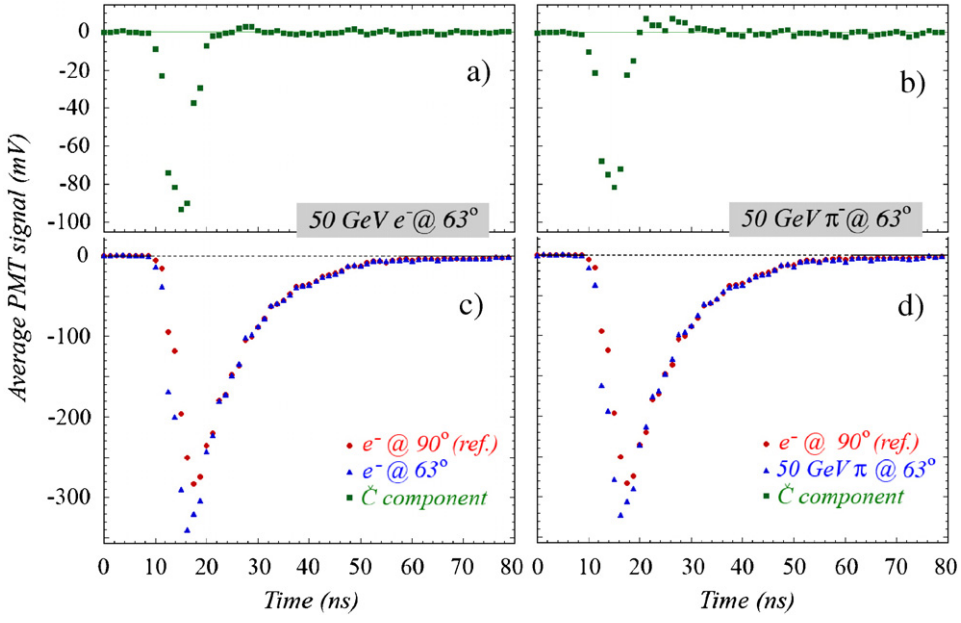

Fig. 13. Time structure of the signals from 50 GeV electron showers in the lead tungstate crystals, measured with detectors located at 90° and 63° with respect to the beam line, for 50 GeV electron (c) and pion (d) showers. The top graphs (a and b) show the difference between the time structures recorded at the two different angles, for the electrons and pions, respectively.

However, there is a very significant difference in the *leading* edge of the pulses. The ones measured in the 63° geometry (Fig. 4) exhibit a steeper rise than the ones from the calibration geometry (Fig. 3). Figs. 13a and b show the result of subtracting the latter pulse shape from the "63°" one: the pulses recorded in the 63° geometry contain an additional "prompt" component of the type one would expect from Cherenkov light. In the case of the electron showers, this additional component represents ~11% of the total signal. For comparison, we recall that the forward/backward asymmetry measurements led us to conclude that the signals from PMT B contained, on average, 9% of Cherenkov light.

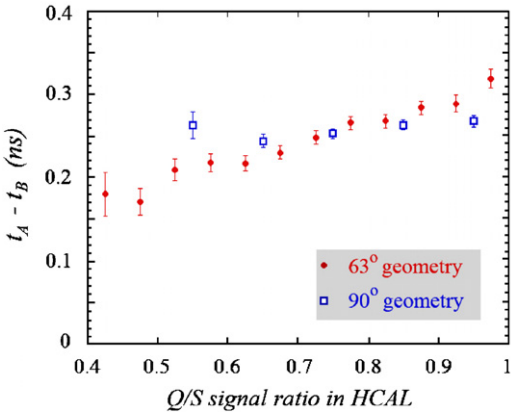

Fig. 14. The difference between the times at which the signals from the two PMTs viewing the light produced in the $PbWO_4$ ECAL reach 50% of their amplitude values, as a function of the fraction of Cherenkov light produced in the showers generated by 50 GeV π^+. This fraction is derived from the Q/S signal ratio in the fiber section of the calorimeter system. Results are given for both geometries used in these studies, described in Figs. 3 and 4.

We have also used these time structure measurements to verify our earlier statement (Section 4.1) that the signal asymmetry $(B-A)/(B+A)$ that was observed when the crystal matrix was rotated from $\theta = 90°$ (Fig. 3) to $\theta = 63°$ (Fig. 4) was the result of Cherenkov radiation, and not of differences in the geometrical acceptance for the scintillation light. Fig. 13 shows that all Cherenkov light is concentrated in the early part of the pulse. Therefore, by integrating the charge from $t = 25$–70 ns, a pure scintillation signal is obtained. We measured that the B/A signal ratio for such pure scintillation signals changed by less than 0.5% when the crystal matrix was rotated.

Fig. 13b shows that the pion signals also exhibit a prompt component, which represents, on average, a somewhat smaller fraction of the total signal than in the case of the electrons. We have studied the possible application of differences in the time structure of these pion signals to determine the Cherenkov component of the light produced in the crystal calorimeter, in a similar way as we used the measured forward/backward asymmetry (Section 4.1). To this end, we used the time at which the calorimeter signal reached half of its amplitude value. The larger the relative contribution of Cherenkov light, the earlier this threshold was reached. Since the contribution of Cherenkov light to the signals from the downstream PMT (B) was larger than that from the upstream PMT (A), we should thus expect the *difference* between the times at which the two signals reach 50% of their amplitude level $(t_A - t_B)$, to be a measure for the fraction of Cherenkov light in the signals from the crystal calorimeter.

Fig. 14 shows this difference, for 50 GeV π^+ showers, as a function of the fraction of Cherenkov light, derived from the Q/S signal ratio measured in the fiber section of the calorimeter. The time difference $t_A - t_B$ increases indeed with this fraction. In order to check the significance of this

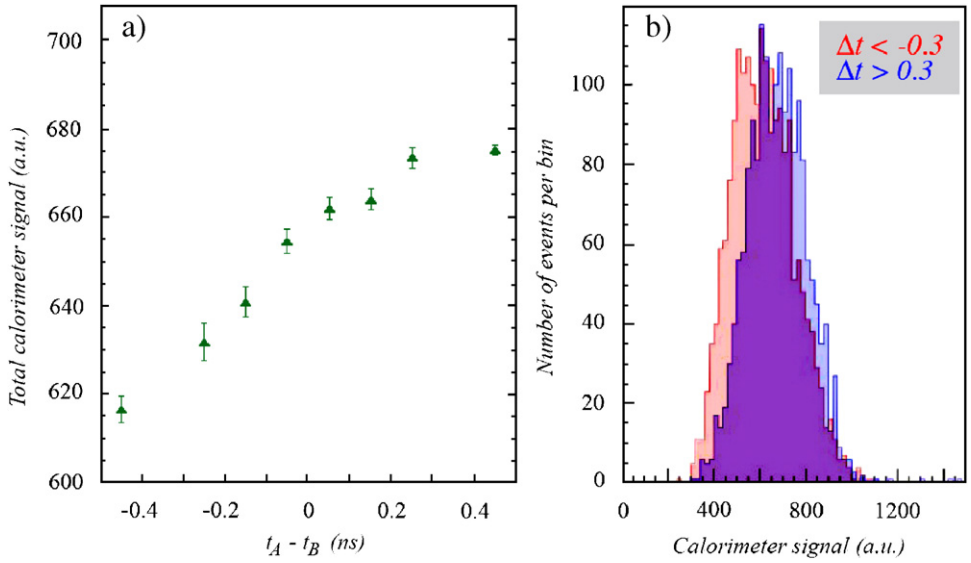

Fig. 15. Average total calorimeter signal for 50 GeV π^+, as a function of the difference between the times at which the signals from the upstream and downstream PMTs reading out the crystal ECAL reach 50% of their amplitude values (a). Diagram b shows the total scintillator signal distributions for two subsamples of events, selected on the basis of this time difference.

result, we also repeated this analysis for the measurements done with the same particles (50 GeV π^+) in the calibration geometry (Fig. 3). The results, shown as squares in Fig. 14, indicate no significant dependence on the Cherenkov fraction in the latter (90°) setup.

As in the case of the forward/backward asymmetry, only events depositing at least 10 GeV in the crystal calorimeter section were considered in these analyses, and therefore the results from Figs. 14 and 8 may be directly compared to each other.

We have also studied the correlation between this time difference and the total calorimeter signals. The results are shown in Fig. 15a, which shows the sum of the signals from ECAL B and the HCAL scintillating fibers, as a function of $t_A - t_B$, for 50 GeV π^+ showers that deposited at least 10 GeV in the ECAL (early starters). Fig. 15b shows these total signal distributions for two subsets of events, selected on the basis of the time difference $t_A - t_B$. These results may be directly compared with those depicted in Figs. 11b and 10d, which concern a similar analysis on the basis of the forward/backward asymmetry. We conclude that the time structure of the crystal signals offers equally valuable opportunities for unraveling the crystal signals into their scintillation and Cherenkov components, and thus of an event-by-event measurement of f_{em} as the directionality of the light production.

5. Conclusions

We have measured the contribution of Cherenkov light to the signals from electrons, muons and hadrons in an electromagnetic calorimeter made of lead tungstate crystals. In the chosen geometry, which was optimized for detecting this component, information about this contribution was obtained from the forward/backward asymmetry in the signals and from their time structure. For single particles traversing the calorimeter (muons, pions), the Cherenkov contribution was measured to be ~20%. The measurements for em showers indicated contributions at about half that level, since a substantial fraction of the signal is in that case typically caused by isotropically distributed shower particles. The contribution of the Cherenkov component to the signals from pion showers fluctuated strongly from event to event. The Cherenkov/scintillor signal ratio in the crystals was found to correlate well with that measured in the dual-readout calorimeter that served as the hadronic section in these measurements. It could also be used to determine the electromagnetic fraction of the pion showers and thus improve the hadronic calorimeter performance.

It should be emphasized that this improvement was far from optimal. Figs. 10d and 15b indicate that the precision with which the Cherenkov/scintillator signal ratio (and thus the em shower fraction) could be measured in individual events was very limited, given the substantial overlap between the total signal distributions for the different event samples. This should come as no surprise, given the minuscule effects that were exploited in this study: a forward/backward asymmetry smaller than 5% and 200 ps effects on the signal rise time. Substantial improvements may be expected in dedicated crystals designed to maximize the precision with which the Cherenkov/scintillator signal ratio can be measured. We are working towards this goal, inspired by the results presented here. This paper is primarily intended to demonstrate the feasibility of applying the dual-readout principles in a crystal calorimeter.

Acknowledgments

The studies reported in this paper were carried out with $PbWO_4$ crystals made available by the PHOS group of the ALICE Collaboration. We sincerely thank Drs. Mikhail Ippolitov and Hans Muller for their help and generosity in this context. We thank CERN for making particle beams of excellent quality available. This study was carried out with financial support of the United States Department of Energy, under Contract DE-FG02-95ER40938.

References

[1] R. Wigmans, Calorimetry—Energy Measurement in Particle Physics, International Series of Monographs on Physics, vol. 107, Oxford University Press, Oxford, 2000.
[2] N. Akchurin, et al., Nucl. Instr. and Meth. A 536 (2005) 29.
[3] N. Akchurin, et al., Nucl. Instr. and Meth. A 537 (2005) 537.
[4] N. Akchurin, et al., Nucl. Instr. and Meth. A 533 (2004) 305.
[5] N. Akchurin, et al., Nucl. Instr. and Meth. A 582 (2007) 474.
[6] O. Ganel, R. Wigmans, Nucl. Instr. and Meth. A 365 (1995) 104.
[7] N. Achurin, et al., The Response of CMS Combined Calorimeters to Single Hadrons, Electrons and Muons, CMS Internal Note 2007/012, 2007.
[8] R. Wigmans, Nucl. Instr. and Meth. A 572 (2007) 215.